Journal of Neurochemistry

JOURNAL OF NEUROCHEMISTRY | 2015 | 135 | 368–380 doi: 10.1111/jnc.13208

ORIGINAL ARTICLE

Chandipura virus perturbs cholesterol homeostasis leading to neuronal apoptosis

Sourish Ghosh, Sriparna Mukherjee and Anirban Basu

National Brain Research Centre, Manesar, Haryana, India

Abstract

Chandipura virus (CHPV; genus Vesiculovirus, family Rhabdoviridae) induces neuronal death through the Fas-mediated extrinsic apoptosis pathway. What propels this apoptosis remains unclear, although oxysterols have been reported to be key players in neurodegeneration. In our study of CHPV-infected brain samples, we observed over-expression of genes such as apolipoprotein E, Cyp46a1, Srebf-1 and Nsdhl. This backs up the hypothesis that CHPV replication demands cholesterol that is supplied by apolipoprotein E through low density lipid receptors, lipid metabolism being pivotal for viral replication. We were able to illustrate this with over-expression of low density lipid receptors in CHPV-infected neurons. An upsurge of cholesterol concentration has been observed in neurons, triggering the expression of Cyp46a1 enzyme and culminating into the conversion of cholesterol to 24(*S*)-hydroxycholesterol. Increased 24(*S*)-hydroxycholesterol concentration is toxic to neurons, propelling neuronal apoptosis through the Fas-mediated extrinsic apoptosis pathway. For the first time, perturbation of cholesterol homeostasis in brain is shown to be utilized by the viruses for both maturation and the release of its matured virions outside the cells for continuous neuropathogenesis.

Keywords: Chandipura virus, cholesterol homeostasis, neuronal apoptosis.

J. Neurochem. (2015) **135**, 368–380.

Cover Image *for this issue: doi: 10.1111/jnc.12908.*

Chandipura virus (CHPV) belongs to the family *Rhabdoviridae* in the order *Mononegavirales* of genus *Vesiculovirus*. As per reports, CHPV has been ranked among the emerging human pathogens in the Indian subcontinent with a fatality rate of around 55–77% (Jadi *et al.* 2010; Menghani *et al.* 2012; Mondal *et al.* 2012). CHPV is predominantly neurotropic to children below 15 years who show symptoms similar to encephalitis such as high grade fever, vomiting, altered sensorium, generalized convulsions, decerebrate posture and grade IV coma (Balakrishnan and Mishra 2008; Gurav *et al.* 2010). Sand fly of *Phlebotomus* spp. and *Sergentomyia* spp. are the major vectors of CHPV evidenced during the outbreaks in recent years (Depaquit *et al.* 2010; Menghani *et al.* 2012). CHPV has a (−) stranded RNA as its genome and is an enveloped virus with an approximate length of 11 kb comprising of 5 genes that translates the following proteins-glycoprotein (G), matrix protein (M), nucleoprotein (N), phosphoprotein (P), and large polymerase (L) protein. These proteins at various stages of viral life cycle help the virus to survive in the host system (Giorgi *et al.* 1983; Barr *et al.* 2002; Basak *et al.* 2007; Cherian *et al.* 2012). Among these, the N and P proteins work in tandem in the viral replication process within the host (Basak *et al.* 2007; Mondal *et al.* 2012; Kumar *et al.* 2013).

In our previous report we have shown that CHPV induces neuronal apoptosis through the Fas-mediated extrinsic apoptosis pathway (Ghosh *et al.* 2013). Neurotropic viruses find their safest place to replicate in the neurons since they do not get cleared away faster as in the peripheral system (Iannacone *et al.* 2010; Nair *et al.* 2014). In neurons, viruses regulate the host metabolic pathways in order to maintain their life cycle within them. On maturation, viruses influence host mechanisms in order to induce apoptosis. This facilitates the release of matured virions outside the cells, helping advance their infection strategy. As an approach to antiviral therapeutics, therefore, it becomes inevitable to identify the fundamental dependencies of the virus within the host. Thus, in case of CHPV, the primary question to address was what are the factors that help it to induce this neuronal apoptosis?

Received March 10, 2015; revised manuscript received June 18, 2015; accepted June 22, 2015.

Address correspondence and reprint requests to Anirban Basu, National Brain Research Centre, Manesar, Haryana 122051, India. E-mail: anirban@nbrc.ac.in

Abbreviations used: 24(*S*)-OHC, 24(*S*)-hydroxycholesterol; ApoE, apolipoprotein E; CHPV, Chandipura virus; Cyp46a1, cholesterol 24-hydroxylase; Nsdhl, sterol-4-alpha-carboxylate 3-dehydroge-nase, decarboxylating; Srebf-1, sterol regulatory element-binding transcription factor 1.

Perturbation of cholesterol homeostasis in the brain has been observed in various cases of neurodegenerative diseases that leads to neuronal apoptosis (Lahiri 2004; Karasinska and Hayden 2011). Accumulation of cholesterol in excess is often not tolerated by neurons. In such instances, they undergo apoptosis as a result of the production of toxic oxysterols (Brugg *et al.* 1996; Taniwaki *et al.* 1999; Movsesyan *et al.* 2002; Stoica *et al.* 2003; Perry and Ridgway 2006; Ngo and Ridgway 2009). On the other hand, cholesterol and lipids are important components of the viral structure that are required for their maturation (de Vries *et al.* 1998; Nakai and Kamiguchi 2002; Kendall *et al.* 2005; Das *et al.* 2010; Talekar *et al.* 2011). It has also been reported previously that cholesterol uptake in neurons increases during viral infection (Jan *et al.* 2000; Ogawa *et al.* 2009; Grove and Marsh 2011). In this study, we demonstrate that viruses target cholesterol homeostasis not only for their maturation within their host but also induce apoptosis for successful release outside the cell. Our study opens the possibility of finding new therapeutic targets that can be taken into consideration for blocking the progression of not only CHPV infection in brain but also for other neurotropic viruses.

Materials and methods

Ethics statement

All animal experiments were approved by the Institutional Animal and Ethics Committee of the National Brain Research Centre (approval no. NBRC/IAEC/2012/70). The animals were handled in strict accordance with good animal practice as defined by the CPCSEA, Government of India.

Virus and cells

CHPV (strain no. 1653514 isolated from human patient in Nagpur, 2003; kindly provided by Prof. D.J. Chattopahyay (D.J.C.), University of Calcutta) was propagated in Vero E6 cell line (Balakrishnan and Mishra 2008). The titer of the virus was found to be 3×10^5 pfu/mL. Vero E6 cells (kind gift from Dr D. P. Sarkar, Delhi University (South Campus), India) and Neuro2a (obtained from National Centre for Cell Science, Pune, India.) were grown at 37°C in Dulbecco's modified Eagle's medium (DMEM) supplemented with 3.5% sodium bicarbonate, 10% fetal bovine serum and penicillin/streptomycin. Staurosporine was used as a positive control for inducing apoptosis in Neuro2a cells at a concentration of 1 μM for 6 h.

Animal treatment

CHPV infection model was developed in 10 day postnatal BALB/c mouse pups (obtained from The Jackson Laboratory, Bar Harbor, Maine, USA) and it has been observed that the infection occurs in the animals without having a sexual bias. Hence, in our experiments, we used both male and female mouse pups. Animals used for the experiments were always kept with mother for milk feeding. For each experiment the animals were divided into two groups- Mock-infected and CHPV-infected in each group consisted of three animals. CHPV group was injected with 50 μL of virus (approximately 1.5×10^4 pfu) while the mock-infected animals were injected with phosphate-buffered saline (PBS) intraperitoneally. CHPV-infected animals succumbed by 76–92 h post-infection. Animals of Control group were also killed at the same time point. Brains were excised after repeated transcardial perfusion with ice-cold 1× PBS followed by tissue fixation using 10% Paraformaldehyde (PFA).

Primary neuron culture

Cortical neurons were cultured following previously published protocol (Ghosh *et al.* 2009). Cells were plated at a density of 3×10^5 cells/cm^2 and 10^4 cells/cm^2 onto poly-D-lysine-coated 60 mm culture plates and 96 well plates, respectively (Nunc, Roskilde, Denmark). After 48 h of incubation at 37°C, the serum containing medium was removed. Cells were incubated with serum free media for 4 h with antibiotics alone. For experimental treatments, the resting medium was exchanged for DMEM with N2 and B27 supplements, 25 mM KCl, and antibiotics.

Plaque assay for growth kinetic study of CHPV

Cell culture supernatant was used for plaque assay by serial dilution. Plaque assay was performed as per previously published protocol (Ghosh *et al.* 2013).

Quantitative PCR array

Total cellular RNA from whole brain tissue was extracted using Tri reagent (Sigma, St Louis, MO, USA). One step cDNA synthesis was done using RT^2 First Strand Kits (SA Biosciences, Valencia, CA, USA). cDNA were then subjected to mouse Lipoprotein Signaling & Cholesterol Metabolism PCR Array (SA Biosciences) as per manufacturers instruction on a ABI Prism 7500 sequence detection system (Applied Biosystems, Waltham, MA, USA). The real-time PCR results were analyzed as per user manual guidelines (Mayoral *et al.* 2008).

Immunoblotting

Protein isolation from both tissue and cells were done as mentioned elsewhere (Ghosh *et al.* 2013). Primary antibodies against Caspase-8 (Abcam, Cambridge, MA, USA), pro & cleaved Caspase-3 (Cell Signaling, USA a kind gift from Dr Ranjit Giri, NBRC), CHPV N & P (kind gift from Prof D.J.C.) at (1 : 1000) and low density lipid (LDL) receptor (Abcam), at (1 : 500) were used for studying the expression levels of respective proteins. The blots were processed for development using chemiluminescence reagent (Millipore Corporation, Bedford, MA, USA). The images were captured and analyzed using Chemigenius Bioimaging System (Syngene, Cambridge, UK). To determine equivalent loading of samples the blots were stripped and reprobed with β-Actin (Sigma-Aldrich, St. Louis, MO, USA).

Immunohistochemistry/cytochemistry

Immunohisto/cytochemistry was performed following previous published protocol (Ghosh *et al.* 2013). Primary antibodies against neuronal marker Microtubule-associated protein-2 (MAP-2) and Glial Fibrillary Acidic Protein (Chemicon, Temecula, CA, USA), Caspase-3 (Chemicon), LDL receptor (Abcam), CHPV N protein (A kind gift from Prof. D. J. C.) at (1 : 500 dilutions) were used to check the expression levels of the respective proteins. Post-staining sections were mounted with DAPI (4′,6-diamidino-2-phenylindole) (Vector Burlingame, CA, USA), observed under a Axio Observer.Z1 Fluorescence microscope (Zeiss, Oberkochen, Germany) and

images were captured with AxioCam MRm. Sections were primarily captured at ×40 magnification, while inset images were captured at ×60 for details. Image acquisition was done with Zen pro 2011, Oberkochen, Germany. We used Adobe Photoshop 7.0, San Jose, CA, USA for adjusting the contrast and brightness of the images.

Determination of cell viability

Primary neurons were plated onto separate 96-well plates in triplicate followed by Methyl-beta-cyclodextrin (MBC) (Sigma-Aldrich) (of various dilutions 1, 3, 5, 7 and 10 mM) along with proper controls for checking the cellular toxicity of the chemicals. MTS (3-(4,5-dimethylthiazol-2-yl)-5-(3-carboxymethoxyphenyl)-2-(4-sulfophenyl)-2H-tetrazolium) assay was conducted hereafter as mentioned elsewhere (Ghosh *et al.* 2013).

Terminal deoxynucleotide transferase-mediated dUTP nick-end labeling assay

Neuro2a cells were plated at a density of 5×10^4 cells/well of eight-well chamber slides (Nunc) and treated with 24(*S*)-hydroxycholesterol (24(*S*)-OHC) (Enzo Lifesciences, Farmingdale, NY, USA) and post-treatment were analyzed for cell death analysis using Cell Death Detection Kit, TMR red (Roche, Penzberg, Upper Bavaria, Germany) as per previously used protocol from our lab (Ghosh *et al.* 2013).

Real-time PCR assay (qPCR)

RNA from whole brain tissue or primary neuronal cells was extracted using Trizol reagent (Sigma). cDNA synthesis was performed using advantage RT-PCR Kit (Clontech, Mountain View, CA, USA) and run on a ABI Prism 7500 sequence detection system (Applied Biosystems). The forward and reverse primers used in qRT-PCR are enlisted in Table S2. The results were normalized with GAPDH (Glyceraldehyde 3-phosphate dehydrogenase).

Total cholesterol assay

Lipid extraction from brain tissue and Neuro2a cells were done by Folch Process (Folch *et al.* 1957). Samples were then analyzed using total cholesterol assay kit (LiquiMAX Cholesterol SLR, Avecon a kind gift from Dr N. R. Jana, NBRC) which followed CHOD/PAP Trinder's Method.

24(*S*)-Hydroxycholesterol measurement by 24(*S*)-hydroxycholesterol ELISA kit

Lipid was extracted from brain tissue and Neuro2a cells and run the samples along with standards supplied with the kit as per the user manual supplied with 24(*S*)-Hydroxycholesterol ELISA Kit (Enzo Lifesciences). Optical density (OD) was measured at 450 nm.

Cyp46a1 ELISA assay

Protein was extracted from both brain tissue and Neuro2a cells and run the samples along with the standards supplied with the kit as per the user manual supplied with Cyp46a1 ELISA Kit (Mybiosource, San Diego, CA, USA). OD was measured at 450 nm.

Nile red staining

Nile Red (Sigma-Aldrich) as per the manufacturer's instructions was dissolved in methanol at 1 mg/mL and kept in 4°C (in dark). After tissues sections were stained with anti-MAP-2 (neuronal marker) and CHPV N as mentioned previously, a working dilution of 1 : 1000 was prepared fresh in PBS and incubated for 15 min. After the incubation, sections were mounted with DAPI as mentioned previously. A similar protocol was followed in case of counter-staining with LDLr and Caspase-3.

Knockdown of LDL receptor and Cyp46a1

Endonuclease-prepared short-interfering RNA (esiRNA) against mouse LDL receptor and Cyp46a1 and scrambled esiRNA Enhanced Green Fluorescent Protein (EGFP) were designed and synthesized by Sigma-Aldrich (Gimenez-Barcons *et al.* 2007). 10 μM of esiRNA was used for transfection using Lipofectamine RNAi max (Invitrogen, Carlsbad, CA, USA) according to the manufacturer's protocol. Briefly, Neuro2A cells were seeded and maintained in sets of three at 37°C and 5% CO_2 and when the cells were 70–80% confluent, they were transfected in Opti-MEM (Invitrogen) for 6 h after which fresh 5% DMEM was added to the cells for 24 h.

Statistical analysis

Data were compared between groups using unpaired t-test using GrapPad Prism 6, La Jolla, CA, USA software. All data were considered to be statistically significant if p value < 0.05 denoted by * and highly significant if p value < 0.01 denoted by #.

Results

Chandipura virus selectively infects neurons in brain

Previously from our lab CHPV has been reported to induce neuronal death through Fas-mediated extrinsic apoptosis pathway (Ghosh *et al.* 2013). We were inquisitive about the target cells of CHPV in the brain. Hence, we double immunostained the brain sections from both CHPV and its corresponding mock-infected ones with CHPV N protein (as a marker for CHPV) along with either MAP-2 (neuronal marker) (Figure S1a) or GFAP (glial cell marker) (Figure S1b). It was observed that CHPV N showed co-localized expression along with MAP-2 but not with GFAP. This proved that CHPV replicates selectively in neurons.

CHPV requires cholesterol for matured virion formation

Previously MBC has been applied to remove cholesterol from cultured cells (Ohtani *et al.* 1989; Kilsdonk *et al.* 1995). Water-soluble MBC has been known to form soluble inclusion complexes with cholesterol, which enhances its solubility in aqueous solution (Pitha *et al.* 1988). In order to check its toxicity towards primary neurons we used various dilutions to treat them for 24 h and analyzed them by MTS assay (Fig. 1a). Both 3 & 5 mM concentrations were able to maintain the survivability of the cells for 24 h approximately to 100%. Thus we used the 3 mM concentration of MBC to pre-treat the cells prior to CHPV infection at 37°C for 30 min. Real-time PCR analysis (qPCR) of MBC treated cells showed no significant change in expression levels of CHPV N & P proteins post-CHPV infection (Fig. 1b) that indirectly implied CHPV's

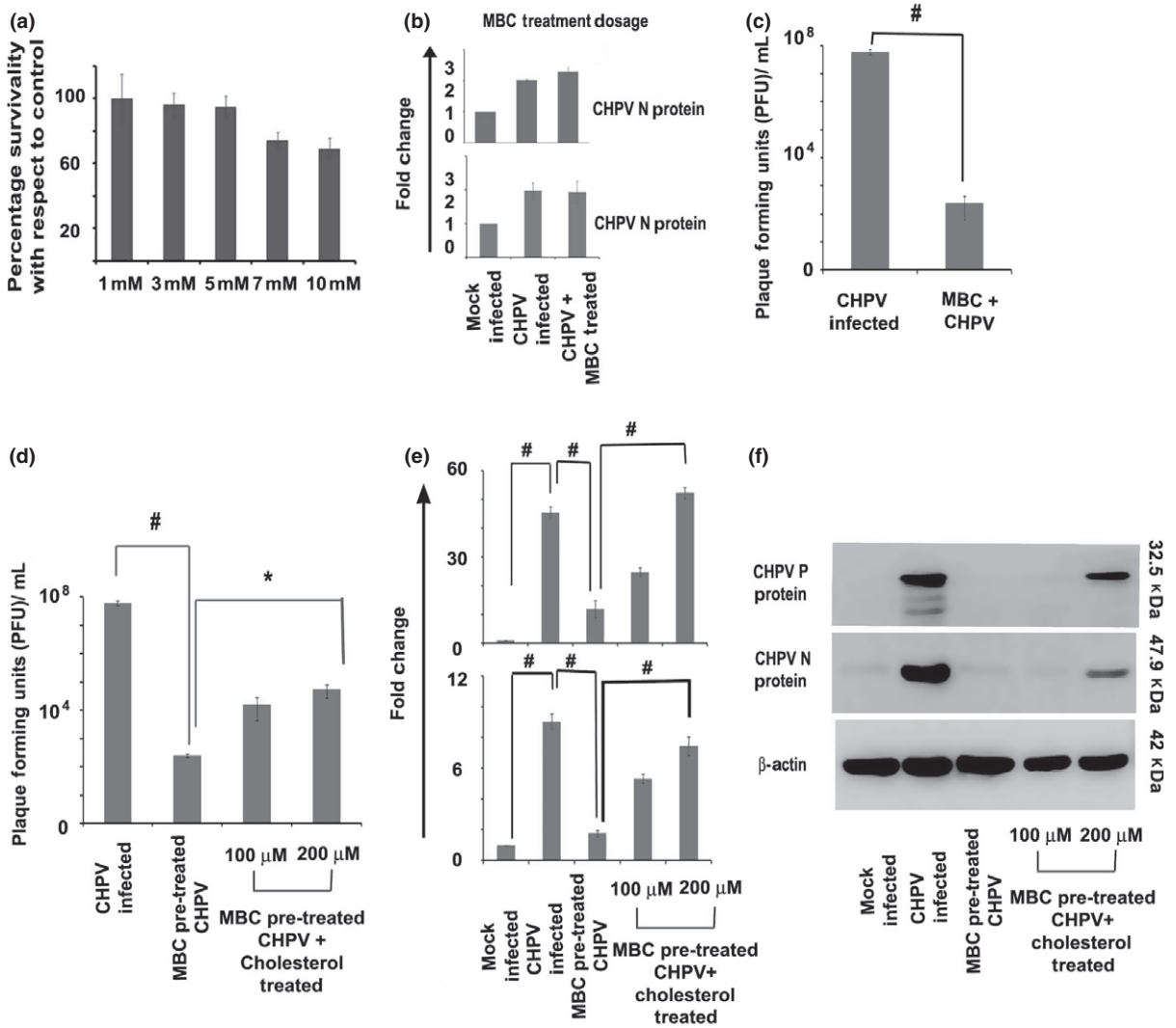

Fig. 1 Viral envelope contributes to virulence of Chandipura virus (CHPV). Representative plot (a) shows percentage survivability score of MTT assay to estimate the optimum treatment concentration of MBC on primary neuron culture for 24 h. Percentage survivability score was calculated as (%) = (A_{570} nm of dying or dead cells/A_{570} nm of live cells) × 100. MBC treatment of 3 mM and 5 mM were able to restore almost 100% survival (n = 5). 3 mM MBC was used to pre-treat primary neurons to deplete cholesterol from the cell culture before infecting them with CHPV. Real-time PCR (qPCR) analysis for CHPV P & N protein (which work in tandem for CHPV replication process), respectively, showed no significant fold change in expression upon MBC treatment in the representative plots when compared with only CHPV-infected samples (b) (n = 5). Virulence of MBC treated matured virions was analyzed using plaque assay. Representative plot in (c) shows pfu/mL for CHPV-infected and CHPV-Infected + MBC-treated sample (n = 5). There was significant reduction in pfu in case of MBC treated sample implying reduction in virulence of the sample. Supernatant of CHPV-infected primary neuron culture was pre-treated with 3 mM MBC for 30 min at 37°C followed by incubation with 100 and 200 μM cholesterol to restore the depleted viral envelope for 1 h at 37°C in two independent treatment groups. Post-treatment the treated groups along with a control set of untreated CHPV was used to infect primary neuron culture. 12 h post-infection period supernatants from all treatment groups was analyzed for virulence measurement using plaque assay. Representative plot in (d) shows pfu/mL for treatment groups: CHPV-infected, CHPV infected + MBC treated, CHPV infected + MBC + cholesterol treated (100 and 200 μM). Significant revival of virulence was observed in the cholesterol treated samples (n = 5). MBC pre-treatment of matured virions hinders CHPV infection of neurons but cholesterol treatment (100 and 200 μM) revived their infectivity and their successful replication within the host. Representative plots (e) and images (f) show qPCR analyses and immunoblots, respectively, of CHPV N & P proteins corresponding to various treatment groups with respect to their controls (n = 5). β-Actin was used as a loading control. $^{*}p < 0.05$, $^{\#}p < 0.01$.

entry into neurons is independent of cholesterol mechanism. Virulence of cell supernatant 12 h post-infection (hpi) was checked. The plaque assay result showed a drastic reduction in viral titer of CHPV obtained from MBC treated cells (Fig. 1c). This substantiated the fact although indirectly that CHPV derive cholesterol from their hosts to form their envelopes for

maintaining virulence. To validate our hypothesis we collected the supernatant from CHPV-infected primary neuron culture and treated it with 3 mM MBC at 37°C for 30 min. This was done to strip off CHPV envelope and then use them for further infection of primary neurons. Again in another treatment group we externally supplied cholesterol (Sigma-Aldrich) of 100 and 200 μM to MBC pre-treated CHPV at 37°C for 1 h to replenish the depleted cholesterol envelope. Thereafter, we used the treatment groups: MBC pre-treated CHPV, MBC pre-treated CHPV + Cholesterol treated (100 and 200 μM) to infect primary neurons. The virulence was checked for all the treatment groups by serially diluting the culture supernatant in plaque assay against a control group of only CHPV infection. Viral titer as previously observed was reduced in case of MBC treated group but the 200 μM cholesterol treated group showed significant revival in virulence (Fig. 1d). Contradictory to the previous qPCR results, there was significant difference in CHPV N & P protein expression between MBC pre-treated CHPV and CHPV-infected groups, which was validated both by qPCR and immunoblot analyses (Fig. 1e and f). Again external 200 μM cholesterol treatment post-MBC treatment of CHPV helped CHPV to make successful replications. These results cumulatively suggest that cholesterol is an essential factor for CHPV to complete its life cycle within the host.

CHPV infection over-expresses ApoE, Cyp46a1, Srebf-1, Nsdhl

Based on our previous result, RNA was extracted from the CHPV-infected brain tissue and their respective mock-infected controls as described in the Experimental Procedures section. It was analyzed by real-time PCR array plates pre-coated with primers for lipoprotein signaling and cholesterol metabolism. Table S1 elucidates the expression levels of 84 genes which were monitored in the analysis. Analysis revealed that genes like apolipoprotein E (ApoE), Cyp46a1, Srebf-1 and Nsdhl were over-expressed consistently in all the three samples with more than fourfold change (the genes are highlighted in Table S1) (Fig. 2a). Among these as mentioned in the table in Fig. 2(a), ApoE was over-expressed by 10-folds (approximately) while the others showed around fourfold over-expression. We also validated the expression levels of the same genes separately in qPCR analysis (here the primers were separately designed as mentioned in Table S2) from CHPV-infected brain tissues as in Fig. 2(b).

ApoE transports cholesterol through LDL receptor

Previously in cases of neurodegeneration, it has been reported that ApoE over-expression is related to increase in cholesterol transport to neurons from astrocytes through LDL receptors (Pfrieger 2003; Kim *et al.* 2009). Initially we observed significant over-expression of LDL receptor in real-time PCR analysis from samples obtained from whole brain tissue ($p < 0.01$) and primary cortical neuron culture ($p < 0.05$) post-CHPV infection (Fig. 3a). The expression level of LDL receptor was also monitored over the time period *in vivo* post CHPV infection. LDL receptor expression level was observed to increase at 4 days post-infection (dpi) when CHPV infection symptoms were

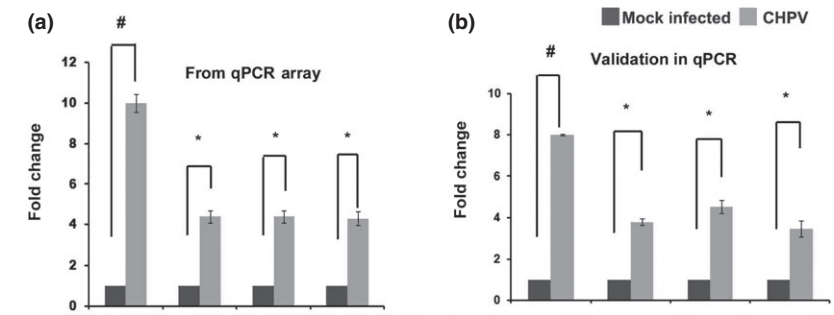

	ApoE	Cyp46a1	Nsdhl	Srebf1
Mock	1	1	1	1
CHPV Gr.1	9.761	4.7437	4.435	4.76
CHPV Gr.2	9.422	3.4702	4.734	3.603
CHPV Gr.3	11.06	5.003	4.081	4.695

	ApoE	Cyp46a1	Nsdhl	Srebf
Mock	1	1	1	1
CHPV Gr. 1	8.004	3.7885	4.525	3.455
CHPV Gr. 2	8.027	4.907	3.29	4.73
CHPV Gr. 3	9.98	3.67	4.76	3.18

Fig. 2 RNA was extracted from Chandipura virus (CHPV)-infected and mock-infected mouse brain samples and analyzed with Lipoprotein Signaling & Cholesterol Metabolism PCR Array in order to find out the genes pertaining to the corresponding metabolism that gets affected (a). Table S1 represents the fold changes of the 84 enlisted genes. Among the enlisted genes, we chose the genes which were consistently showing over-expression in all the CHPV-infected samples with fold change more than 4 (approximately). The table enlists the genes which were over-expressed in CHPV-infected samples with respect to their mock-infected controls. The corresponding graphical representation shows four genes apolipoprotein E (ApoE), Cyp46a1, Nsdhl and Srebf1 were significantly over-expressed in CHPV-infected samples. Analysis was performed using: http://www.sabiosciences.com/pcrarraydataanalysis.php ($n = 3$). Representative plot (b) is a qPCR validation of the over-expressed genes ($n = 3$).

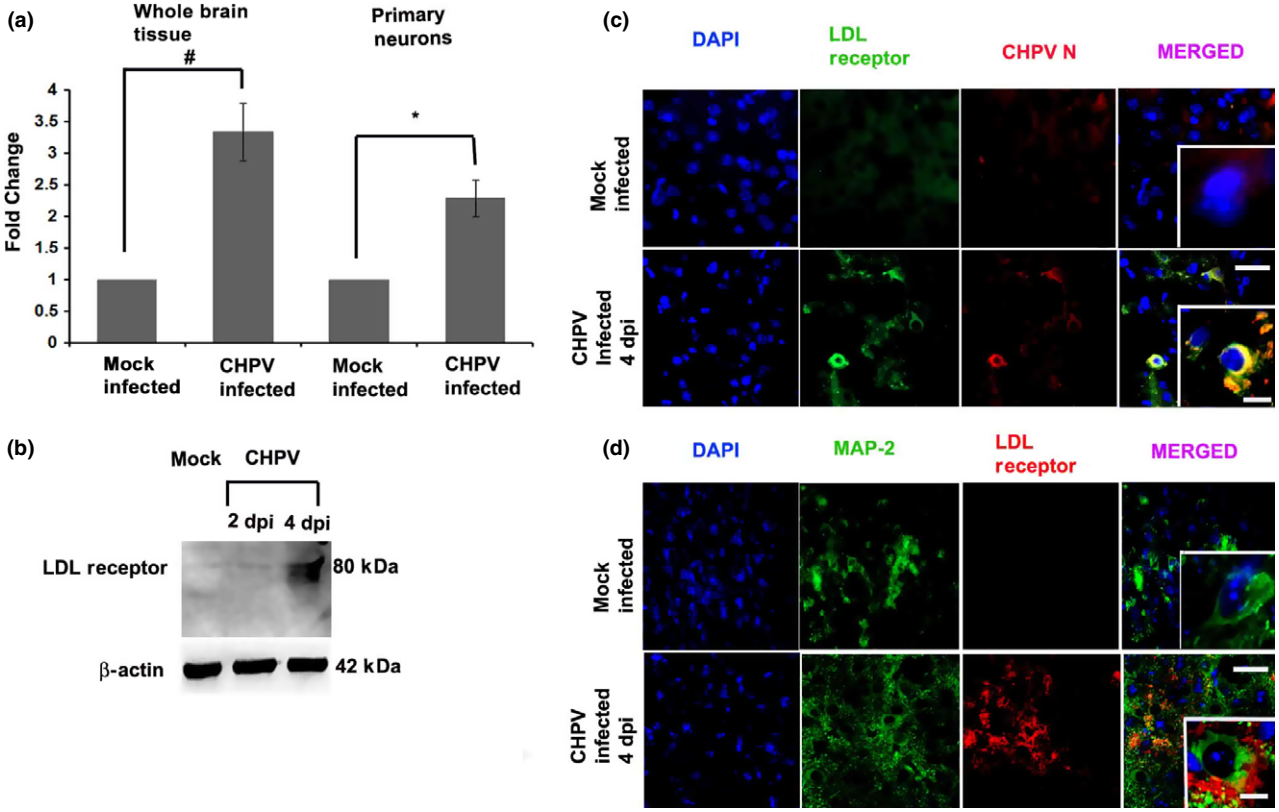

Fig. 3 Low density lipid (LDL) receptor gets over-expressed in Chandipura virus (CHPV)-infected cells. Representative plot (a) shows significant fold changes in real-time PCR analysis of LDL receptor from CHPV-infected whole brain and primary neurons RNA samples with respect to their respective mock-infected controls ($n = 5$). Immunoblot analysis (b) shows expression of LDL receptors from mock-infected, CHPV-infected 2 dpi and 4 dpi whole brain lysates. β-Actin was used as a loading control ($n = 5$). Image panels show double immunohistochemistry staining of LDL receptor/CHPV N (c) and LDL receptor/MAP-2 (d) proteins of mock and CHPV-infected animals (image scale = 20 μm; inset scale = 10 μm) ($n = 5$). Hence the two double staining results prove that LDL receptor expression goes up following CHPV expression specifically in CHPV-infected neurons.

prominent (Fig. 3b). The above data however does not confirm about the expression level of LDL receptors in CHPV-infected neurons. Hence in order to substantiate our hypothesis we performed double immunostaining of LDL receptor/CHPV N (Fig. 3c) and LDL receptor/MAP-2 (Fig. 3d). Both analyses showed co-expression of LDL receptor along with MAP-2 (neuronal marker) and CHPV N protein antibody (CHPV virus marker) that clearly validate the fact LDL receptor is expressed in CHPV-infected neurons.

In order to strengthen our claim that ApoE- LDL receptor association is utilized by neurons to import cholesterol we utilized an *in vitro* model system in Neuro2a cells. We incubated 5 μM ApoE (Cloud Clone, Houston, TX, USA) with 200 μM cholesterol at 37°C for 1 h for proper binding. Prior to treatment we knocked down the expression of LDL receptor with a cocktail of siRNA oligos known as esiLDLr in one of the treatment groups. As a negative control, esiEGFP was also transfected to eliminate the off-target effects of gene knock-down with esiRNAs. Lipofectamine was used as a tranfection reagent in our experiments. As we know lipofectamine are lipid compounds and may induce stress to the cells, we kept a mock-infected lipofectamine group as another control in our immunoblotting analysis. Using proper control groups we pre-treated the cells with ApoE-cholesterol mixture for 30 min at 37°C. Then the respective groups were infected with CHPV and incubated for 12 h before the cells were analyzed for immunostaining (Fig. 4a) and immunoblotting (Fig. 4b). From immunoblotting analysis we observed a significant knockdown in expression of LDL receptor compared to the CHPV and esiEGFP group. Also a twofold inhibition in expression of CHPV marker protein (CHPV N) in the LDLr knockdown group compared to the CHPV and esiEGFP group was observed. Nile Red (9-diethylamino-5H-benzo(α)phenoxazine-5-one), is an uncharged phenoxazone dye whose fluorescence properties varies in response to the polarity of its immediate environment because of a large change in dipole moment upon excitation (Greenspan *et al.* 1985). Nile Red has been frequently used to identify intracellular cholesterol concentration within cells (Mukherjee *et al.* 2007; Kucherak

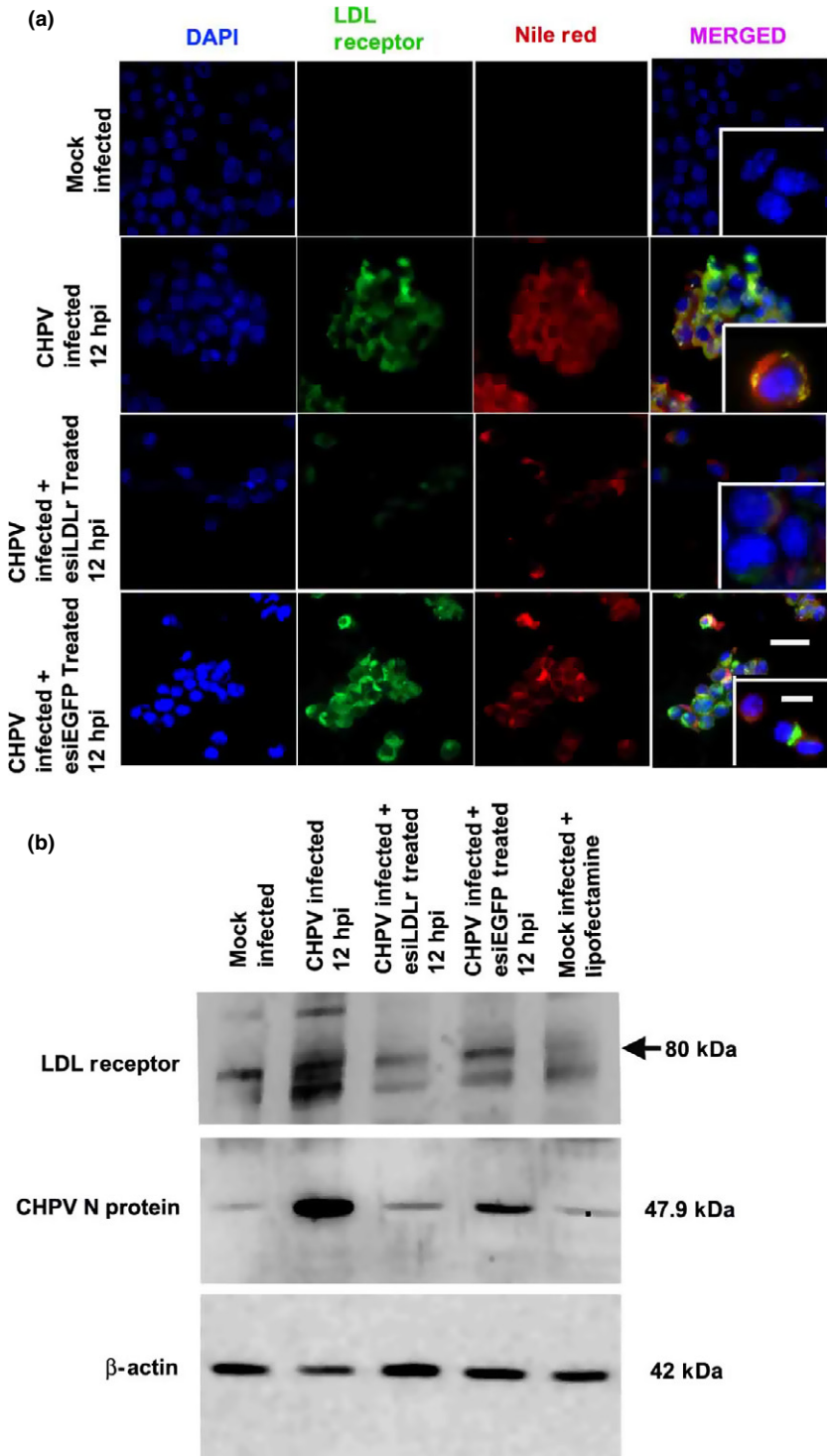

Fig. 4 Low density lipid (LDL) receptor knockdown hindered internalization of externally supplied cholesterol in Neuro2a cells. Cholesterol internalization in neurons happens through apolipoprotein E (ApoE)-LDLr association *in vivo*. In order to verify the role of LDLr *in vitro* system we supplied 200 μM cholesterol and 5 μM ApoE to the cell culture medium post-knocking down the expression of LDLr, hence infected the cells with Chandipura virus (CHPV). The experiment had four treatment groups as: mock-infected, CHPV infected, CHPV infected + esiLDLr treated, CHPV infected + esiEGFP treated (scrambled). Double immunocytochemistry staining of LDLr/Nile Red was performed to analyze the internalization of cholesterol post-CHPV infection. The representative image panels (a) show internalization of externally supplied cholesterol was significantly reduced in the LDLr knockdown treatment group compared to CHPV and scrambled groups (image scale = 20 μm; inset scale = 10 μm) ($n = 3$). Immunoblot analyses (b) show expression of LDLr and CHPV N protein from the similar analysis groups as in (a). β-Actin was used as a loading control ($n = 3$). The immunoblot result shows successful knockdown of LDLr which resulted in reduced internalization of cholesterol as shown in (a). Hence this resulted in reduced CHPV replication as evident from the immunoblot analysis of CHPV N protein.

et al. 2010). Referring to immunostaining analysis LDL receptor knockdown was verified by the decreased expression of LDLr in the knockdown group compared to the CHPV-infected and negative control groups. Along with that, reduction in Nile Red staining in the same knockdown group indicated less cholesterol accumulation within the cells when compared to the CHPV-infected and CHPV-infected esiEGFP groups. The CHPV-infected esiEGFP group showed almost similar results as that of CHPV-infected group in both immunoblotting and immunostaining analyses. These results reflect that with LDLr knockdown cholesterol internalization gets affected.

Hence, the above results corroborate our hypothesis that neurons post-CHPV infection receives cholesterol from astrocytes with ApoE acting as the transporter which binds to the LDL receptor.

Cholesterol concentration increases in neurons post-CHPV infection

We utilized the property of Nile Red that enables it to fluoresce in response to a change in polarity in its environment to measure intracellular cholesterol concentration in CHPV-infected mouse brain. Nile Red was double stained with MAP-2 (Fig. 5a) and CHPV N (Fig. 5b) in 2 and 4 days post-infection (dpi) CHPV-infected mouse sections. The panel images show significant expression of Nile Red stains co-expressed within neurons in both 2 & 4 dpi while with virus in 4 dpi sections. Our hypothesis was further validated from total cholesterol measurement done from a cholesterol quantification assay that showed significant production of cholesterol in the 2 & 4 dpi samples (Fig. 5c). Hence the above two observations validate the fact of increase in intracellular cholesterol post-CHPV infection in neurons.

Cyp46a1 converts cholesterol to 24(*S*)-OHC in neurons

Cyp46a1 has been evidenced to show a fourfold increase in its expression from the real-time PCR array experiment (Fig. 2). We quantified the expression of Cyp46a1 with the help of an ELISA assay. The assay reported a significant rise in Cyp46a1 enzyme in 4 dpi sample (Fig. 5c). Previously it has been reported in several instances that this enzyme is mainly found in neurons and is responsible for converting cholesterol to 24 (*S*)-OHC (Famer *et al.* 2007; Yamanaka *et al.* 2011). We estimated the amount of 24(*S*)-OHC being produced in the brain post-CHPV infection using an ELISA-based assay. The concentration of 24(*S*)-OHC was determined by plotting the OD to the concentration in the standard curve and calculated the concentration in terms of μmol per mg tissue. The concentration was found to be threefold higher in CHPV-infected brain (approximately 15 μM) compared to their mock-infected controls as shown in Fig. 5(c).

24(*S*)-OHC leads to neuronal apoptosis

24(*S*)-OHC has been previously reported to be toxic for neurons which stimulated neuronal death (Kolsch *et al.* 1999; Yamanaka *et al.* 2011). Referring to Fig. 5(c), we investigated the effect of 24(*S*)-OHC on Neuro2a cells using a similar concentration of 15 μM for treatment. Since we solubilized 24 (*S*)-OHC in dimethylsulfoxide (DMSO) we treated our neuronal culture with a similar amount of DMSO as a check for toxicity. Terminal deoxynucleotide transferase-mediated dUTP nick-end labeling (TUNEL) assay determined significant TUNEL positive cells in the 24(*S*)-OHC treated neuronal culture after 24 h of treatment compared to other control samples (Fig. 6a). The TUNEL positive cells in case of 24(*S*)-OHC treatment group showed similar quantification as in

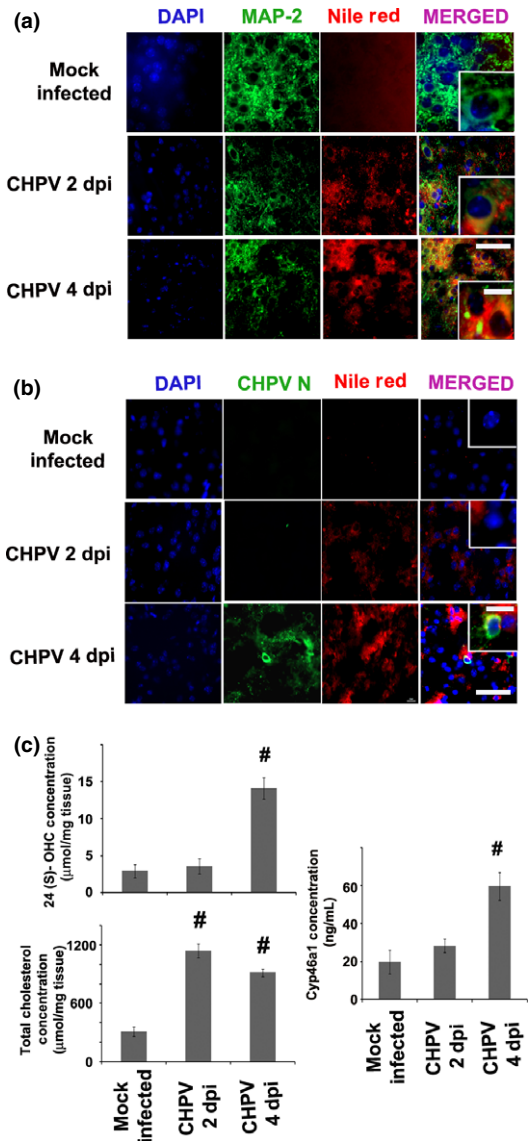

Fig. 5 Nile Red stains intracellular cholesterol accumulation post-Chandipura virus (CHPV) infection. Image panels show double immunohistochemistry staining of MAP-2/Nile Red (a) and CHPV N/ Nile Red (b) of mock and CHPV-infected animals (2 dpi and 4 dpi) (image scale = 20 μm; inset scale = 10 μm) (n = 5). The immunostainings prove that CHPV-infected neurons induce the cholesterol internalization. Cyp46a1 is a neuron specific enzyme which converts cholesterol to a more soluble form as 24(*S*)-hydroxycholesterol (24(*S*)-OHC) for ease of excretion outside the cell. We quantified the amount of total cholesterol, 24(*S*)-OHC and Cyp46a1 produced in the CHPV-infected brain tissue (2 and 4 dpi) compared to their mock-infected controls (c) (n = 5). Significant production of 24(*S*)-OHC was observed in 4 dpi samples which imply the accumulation of the same in brain tissue. Cholesterol concentration was significantly higher compared to their mock-infected controls in both 2 & 4 dpi samples but in 4 dpi the cholesterol concentration was comparatively lower than 2 dpi. Cyp46a1 concentration in 4 dpi samples was significantly higher compared to its mock and 2 dpi-infected samples indicating that accumulation of 24(*S*)-OHC is contributed by enhanced enzyme activity.

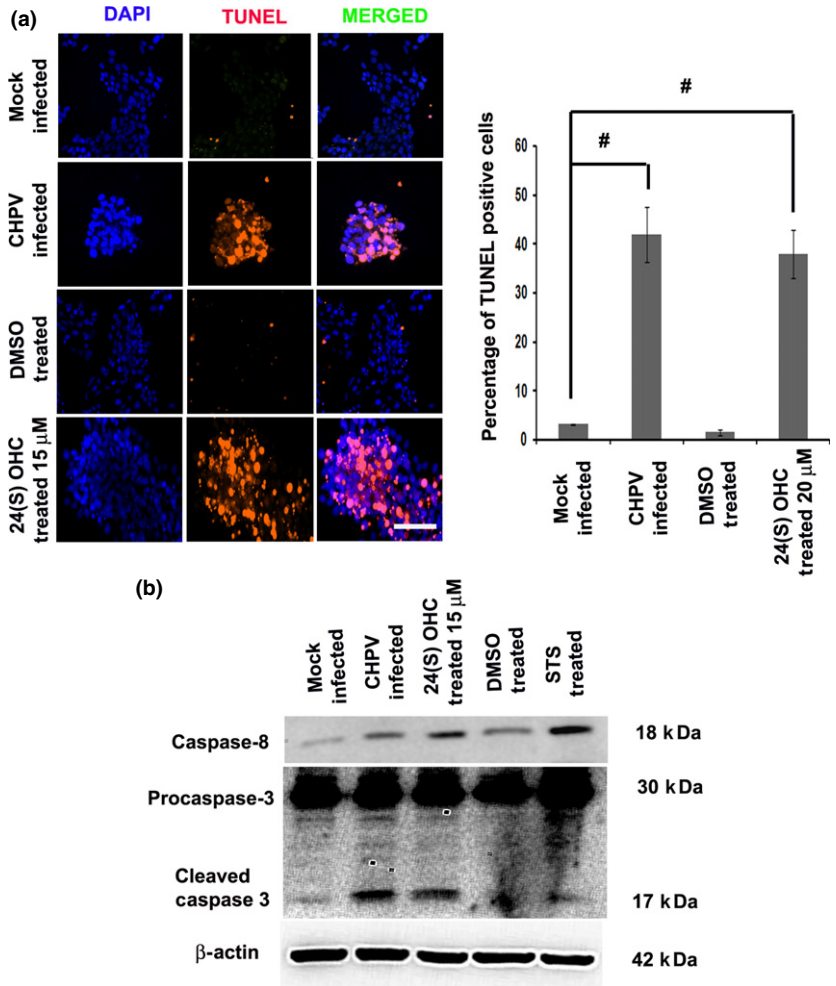

Fig. 6 24(*S*)-hydroxycholesterol (24(*S*)-OHC) induces neuronal apoptosis. Excessive accumulation of 24(*S*)-OHC has been reported to be toxic for neurons and they undergo apoptosis. Image panels in (a) shows terminal deoxynucleotide transferase-mediated dUTP nick-end labeling (TUNEL) analysis of mock infected, Chandipura virus (CHPV)-infected, dimethylsulfoxide (DMSO)-treated and 24(*S*)-OHC-treated (15 μM) Neuro2a cells (image scale = 20 μm). The result shows significant amount of neuronal death with 24(*S*)-OHC comparable to CHPV-infected ones. The adjacent representative plot shows the amount of TUNEL positive cells in each samples ($n = 5$). The *y* axis means: Percentage of TUNEL positive cells = number of TUNEL positive cells/total number of cells × 100. Immunoblotting analyses show expression of Caspase- 8 and pro-& cleaved Caspase-3 in various cell lysate samples of mock-infected, CHPV-infected, 24(*S*)-OHC (15 μM), DMSO and Staurosporine (STS) (1 μM) treated Neuro2a in (b). β-Actin was used as a loading control ($n = 5$). The blot results imply that accumulation of 24(*S*)-OHC in neurons leads to cell death through extrinsic apoptosis pathway.

CHPV-infected group. Neuronal apoptosis was further confirmed from the immunoblot analyses that showed significant expression of Caspase-8, pro & cleaved Caspase-3 from our 24(*S*)-OHC treated sample (Fig. 6b). Staurosporine (1 μM) for 6 h treatment was used as a positive control for the experiment. This helped us to conclude that accumulation of 24(*S*)-OHC induces neuronal apoptosis.

Again to validate our above two findings, we knocked down the expression of Cyp46a1 in Neuro2a with esi-Cyp46a1. Following a similar protocol as LDLr knockdown, all the groups were supplied with a mixture of ApoE-cholesterol and incubated for 30 min prior to CHPV infection. 12 hpi the cells were harvested to extract RNA for qPCR analysis of Cyp46a1 (Fig. 7a), CHPV P (Fig. 7b), protein for Cyp46a1 ELISA assay and lipids to measure the concentration of total cholesterol and 24(*S*)-OHC (Fig. 7c). Figure 7(a) shows a significant knockdown in the expression of Cyp46a1, while Fig. 7(b) shows a fourfold reduction in the expression of CHPV P protein in the Cyp46a1 knockdown group. This certainly points out to the fact that there had been a hindrance in CHPV replication in the absence of Cyp46a1 expression. Cholesterol concentration increased in all the samples except mock-infected group as expected (Fig. 7c). The ELISA results confirmed that CHPV infection propelled the influx of cholesterol within the cells which resulted in production of Cyp46a1 and 24(*S*)-OHC in experimental groups of only CHPV-infected and scrambled esiRNA, but not where Cyp46a1 expression has been knocked down (Fig. 7c). In addition to this, we double immunostained the experimental groups of Cyp46a1 knockdown experiment with Caspase-3/Nile Red (Fig. 7d). We observed that with knockdown of Cyp46a1 although there was significant Nile Red staining indicating the presence of intracellular cholesterol but there was no Caspase-3 expression. Hence it proves although cholesterol was present it was not been converted to 24(*S*)-OHC in the absence of Cyp46a1 enzyme, and thus no neuronal apoptosis was witnessed. On the contrary the CHPV-infected and CHPV-infected esiEGFP groups showed co-localized expression of Caspase-3 & Nile Red. Another significant observation that can be made from Fig. 7(c) and (d) is that although both cholesterol assay and Nile Red staining quantifies intracellular cholesterol content there is an observable difference in the assay estimation and staining. Since Neuro2a cells are adherent cells on undergoing

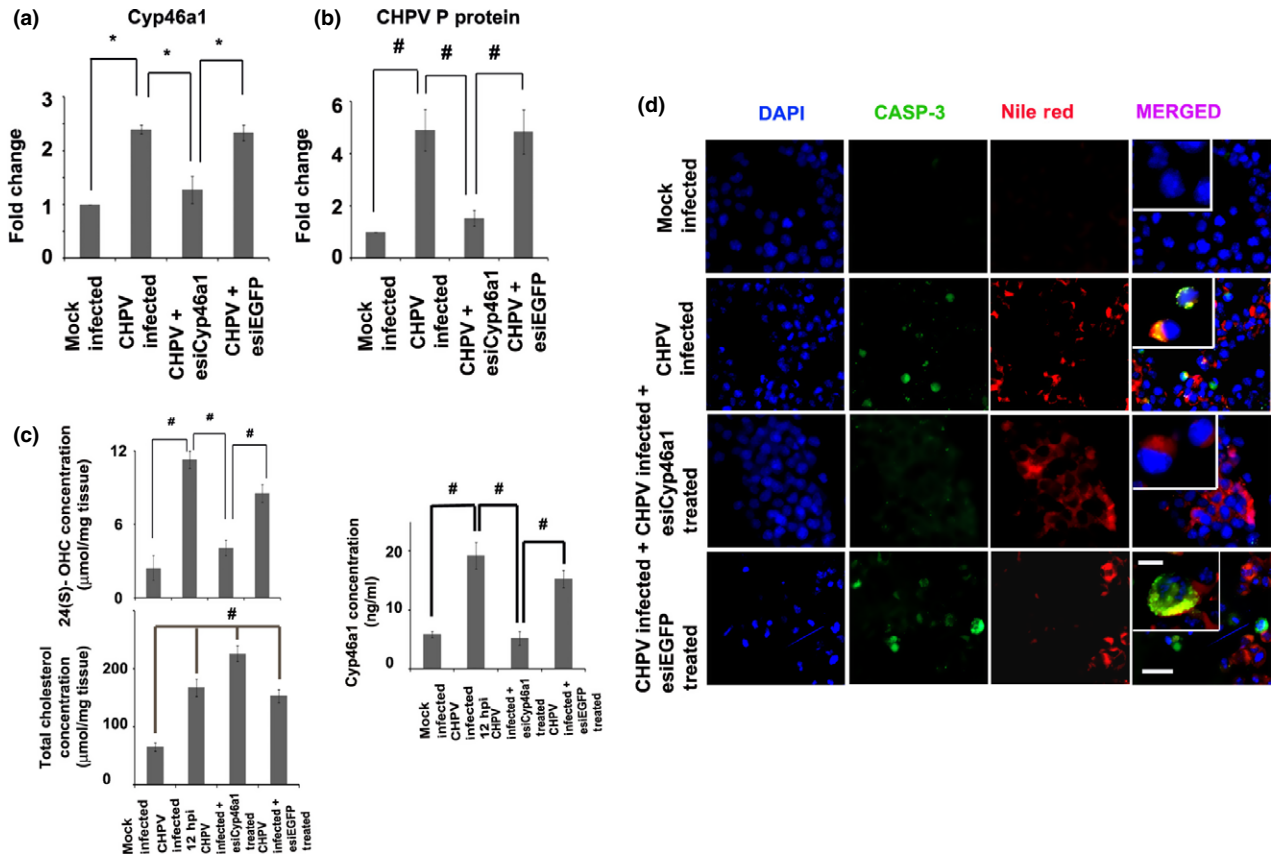

Fig. 7 Cyp46a1 knockdown blocks the conversion of internalized cholesterol to 24(*S*)-hydroxycholesterol (24(*S*)-OHC) in Neuro2a cells. Figure (a) shows expression of Cyp46a1 in qPCR analysis from various treatment groups with respect to their mock-infected controls ($n = 3$). Figure (b) shows expression of Chandipura virus (CHPV) P protein in qPCR analysis from various treatment groups with respect to their mock-infected controls ($n = 3$). The results confirm the knockdown of Cyp46a1 and reduction in CHPV replication in the knockdown treatment group. In order to verify the role of Cyp46a1 *in vitro* system we supplied 200 μM cholesterol and 5 μM apolipoprotein E (ApoE) to the cell culture medium post-knocking down the expression of Cyp46a1, hence infected the cells with CHPV. Effect of Cyp46a1 knockdown in total cholesterol, 24(*S*)-OHC and Cyp46a1 enzyme production was measured (c) ($n = 3$) Significant reduction in Cyp46a1 secretion was observed that contributed to reduced 24(*S*)-OHC accumulation in Cyp46a1 knockdown samples. Total cholesterol showed significant rise in the knockdown samples compared to their corresponding mock-infected ones. In a similar experimental set-up double immunostaining for cleaved Casp-3/Nile Red was performed to verify that Cyp46a1 knockdown reduces the production of 24(*S*)-OHC hence neuronal death was reduced. The representative image panels (d) showing double immunocytochemical staining of cleaved Casp-3/Nile Red of cells belonging to analysis groups of mock infected, CHPV infected, CHPV infected + esiCyp46a1 treated, CHPV infected + esiEGFP treated (scrambled) (image scale = 20 μm; inset scale = 10 μm) ($n = 3$).

apoptosis following viral infection the cells get detached from their adherent surface. In case of performing assay we pulled down those floating cells from the nutrient media while this was not possible in case of immunostaining analysis. Thus, very small amount of cells were available for performing the Nile Red/Caspase-3 co-localization analysis. Hence this explains the observed discrepancy in the result.

Discussion

We previously observed that CHPV is a predominant neurotropic virus and has been evidenced to replicate specifically in neurons in the brain (Figure S1). Cholesterol homeostasis is an important aspect of human physiology. In the peripheral organs, it is maintained by lipoprotein shuttle between liver, intestine and other organs through blood circulation. Cholesterol homeostasis mechanism of peripheral system is totally partitioned from that of brain by the BBB (Blood-Brain barrier) (Pfrieger and Ungerer 2011). Neurons in their developmental phase require high cholesterol diet to build their myelin sheath, synapses, axons and dendrite formation. But as they mature, they shut off cholesterol production (in such large amounts) to conserve their metabolic energy in order to perform other important functions, outsourcing cholesterol synthesis activity to the astrocytes. In a preliminary study, we observed significant accumulation of intracellular

cholesterol within CHPV-infected neurons (Fig. 5). Correlating the fact that viruses utilize lipid metabolism of the host in various stages of their life cycle and our present observation, we explored the possibilities of CHPV manipulating the lipid metabolism in brain (Sun and Whittaker 2003; Ogawa *et al.* 2009; Perera *et al.* 2012).

Figure 1 suggests that cholesterol is an essential component required by CHPV for the development of the viral envelope to maintain its virulence. CHPV manipulates various host genes to bring about this perturbation in the homeostasis. As evidenced in Fig. 2, CHPV internalization within neurons triggers the over-expression of 4 genes: ApoE, Cyp46a1, Srebf-1 and Nsdhl. ApoE, which has been reported in previous studies concerning neurodegeneration (Lahiri 2004; Cao *et al.* 2007; Vance and Hayashi 2010), plays a major role in cholesterol transportation from astrocytes to neurons (Poirier *et al.* 1993; Michikawa *et al.* 2000). This cholesterol transportation from astrocytes to neurons happens with the involvement of proteins such as ApoE, ABCA1, and LDLr (Hirsch-Reinshagen *et al.* 2004; Karasinska and Hayden 2011). Hence, it has been reported that LDLr is the main gateway of neurons for cholesterol entry and ApoE directly binds to LDLr. The LDLr and ApoE binding has been hypothesized to be because of an electrostatic interaction between the hydrophilic lipoprotein receptor module 5 (LR5) and a high-density positively charged region of ApoE (residue 135–150) (Prevost and Raussens 2004). Although there is evidence that the interaction is supported by a tryptophan molecule and a stack of histidine residues, indicating that the interaction is not exclusively an ionic one. LDLr was seen to get over-expressed in CHPV-infected neurons and supports our hypothesis that CHPV propels the import of cholesterol within neurons through the ApoE-LDLr interaction (Fig. 3). Our knockdown experiment related to LDL receptor further validates the phenomenon (Fig. 4). Although cholesterol is mainly imported in neurons from astrocytes through the ApoE-LDLr system, over-expression of genes like Srebf-1 and Nsdhl signifies the in-house cholesterol biosynthesis, which is also regulated by CHPV internalization in neurons (Fig. 2). Since neurons do not allow the presence of excessive intracellular cholesterol, they convert them to more soluble form as 24(*S*)-OHC by an enzyme Cyp46a1 for ease of its excretion (Yamanaka *et al.* 2011). Cyp46a1 has been reported to be largely a neuronal enzyme that has been observed to over express in CHPV-infected brain (Fig. 2). Although the exact mechanism of Cyp46a1 secretion in neurons following CHPV infection is not known but from our results we can hypothesize that any pathogenic condition that stimulates the over accumulation of cholesterol within neurons triggers the Cyp46a1 secretion. Cyp46a1 has been observed to be involved in hydroxylation of cholesterol at 24th carbon position to form 24(*S*)-OHC (Famer *et al.* 2007; Matsuda *et al.* 2013). Also, 24(*S*)-OHC exits neurons either to escape through BBB mediated by CSF or blood circulation or act as a ligand for LXR in astrocytes. In astrocytes, LXR stimulates the transcription of ApoE for enhancement of cholesterol transport that contributes to the cholesterol homeostasis in brain. 24(*S*)-OHC in normal metabolic condition contributes to cholesterol homeostasis in brain but it has been reported that its excessive accumulation is toxic to neurons (Yamanaka *et al.* 2011). Neurons hereafter undergo cell death either through apoptosis or necrotic pathway, but the precise pathway is still not clear. Moreover, as suggested by the recent findings, it mainly depends on the cells' endogenous ability to express caspase-8 (Yamanaka *et al.* 2014). In our experiment, we checked for the probable apoptotic/necrotic genes and found that neuro2a upon being treated with 24(*S*)-OHC expressed both caspase-8 and caspase-3. Hence, in this experiment, neuro2a undergoes apoptosis. As we observed before and in the current study, neurons undergo cell death through extrinsic apoptotic pathway (Fig. 6). Our results were further validated by knocking down the expression of Cyp46a1 that reduced the production of 24(*S*)-OHC and neuronal apoptosis (Fig. 7). In addition to this, we witnessed significant reduction in CHPV replication in the Cyp46a1 knocked down experimental group (Fig. 7). Hence, the accumulation of 24(*S*)-OHC is in direct correlation with the neuronal death that facilitates the release of matured virions outside the cell.

In summary, the perturbation of cholesterol homeostasis in brain is a two-pronged strategy used by CHPV in neuropathogenesis. On one hand, CHPV manipulates the host genes to bring in cholesterol supply to facilitate its envelope formation, while on the other excessive cholesterol being converted to 24(*S*)-OHC brings about neuronal apoptosis to help the process of release of matured viruses outside the cell. In the context of neuropathogenesis, this is a plausible explanation for the strategy adopted by CHPV. But this may not hold true for other hosts, as we know that viruses adopt different infection strategies depending on host and environment. Perturbation of cholesterol homeostasis in brain is a popular topic of discussion in the context of neurodegenerative diseases such as Alzheimer's disease, but its relation to virus-mediated neuropathogenesis is uncommon. There have been reports that discuss the manipulation of cholesterol biosynthesis by neurotropic viruses to perturb the cellular immune response (Mackenzie *et al.* 2007). There is also evidence suggesting that viral replication largely depends on the host cholesterol metabolism (Rothwell *et al.* 2009). Whether the strategy applied by CHPV, which we discussed in this report, might apply to other neurotropic viruses would require investigation. Also, genes pertaining to the lipid metabolism can be interesting targets for future anti-viral therapy.

Acknowledgments and conflict of interest disclosure

We thank Prof D. J. Chattopadhyay, Calcutta University, for providing us with the virus strain and the necessary viral antibodies.

We acknowledge the insightful comments and technical assistance from Dr Bibhabasu Hazra, Mr Kanhaiya Lal Kumawat, and Mr Manish Dogra. The study was funded by a grant from the Department of Biotechnology, Government of India (BT/PR7907/MED/29/702/2013), to AB. AB is also a recipient of Tata Innovation Fellowship (BT/HRD/35/01/02/2014) from the Department of Biotechnology, Government of India. SM is a recipient of DST INSPIRE Fellowship (DST/INSPIRE Fellowship/2014/74). The authors have no conflicts of interest to declare.

All experiments were conducted in compliance with the ARRIVE guidelines.

Supporting information

Additional supporting information may be found in the online version of this article at the publisher's web-site:

Figure S1. CHPV exclusively infects neurons in the brain.

Table S1. Illustrates the fold change of 84 enlisted genes in Mouse Lipoprotein Signaling & Cholesterol Metabolism PCR Array (SA Biosciences, USA) post-CHPV infection with respect to their mock-infected controls.

Table S2. List of Primers which were used.

References

Balakrishnan A. and Mishra A. C. (2008) Immune response during acute Chandipura viral infection in experimentally infected susceptible mice. *Virol. J.* **5**, 121.

Barr J. N., Whelan S. P. and Wertz G. W. (2002) Transcriptional control of the RNA-dependent RNA polymerase of vesicular stomatitis virus. *Biochim. Biophys. Acta* **1577**, 337–353.

Basak S., Mondal A., Polley S., Mukhopadhyay S. and Chattopadhyay D. (2007) Reviewing Chandipura: a vesiculovirus in human epidemics. *Biosci. Rep.* **27**, 275–298.

Brugg B., Michel P. P., Agid Y. and Ruberg M. (1996) Ceramide induces apoptosis in cultured mesencephalic neurons. *J. Neurochem.* **66**, 733–739.

Cao G., Bales K. R., DeMattos R. B. and Paul S. M. (2007) Liver X receptor-mediated gene regulation and cholesterol homeostasis in brain: relevance to Alzheimer's disease therapeutics. *Curr. Alzheimer Res.* **4**, 179–184.

Cherian S. S., Gunjikar R. S., Banerjee A., Kumar S. and Arankalle V. A. (2012) Whole genomes of Chandipura virus isolates and comparative analysis with other rhabdoviruses. *PLoS ONE* **7**, e30315.

Das S., Chakraborty S. and Basu A. (2010) Critical role of lipid rafts in virus entry and activation of phosphoinositide 3' kinase/Akt signaling during early stages of Japanese encephalitis virus infection in neural stem/progenitor cells. *J. Neurochem.* **115**, 537–549.

Depaquit J., Grandadam M., Fouque F., Andry P. E. and Peyrefitte C. (2010) Arthropod-borne viruses transmitted by Phlebotomine sandflies in Europe: a review. *Euro. Surveill.* **15**, 19507.

Famer D., Meaney S., Mousavi M., Nordberg A., Bjorkhem I. and Crisby M. (2007) Regulation of alpha- and beta-secretase activity by oxysterols: cerebrosterol stimulates processing of APP via the alpha-secretase pathway. *Biochem. Biophys. Res. Commun.* **359**, 46–50.

Folch J., Lees M. and Sloane Stanley G. H. (1957) A simple method for the isolation and purification of total lipides from animal tissues. *J. Biol. Chem.* **226**, 497–509.

Ghosh D., Mishra M. K., Das S., Kaushik D. K. and Basu A. (2009) Tobacco carcinogen induces microglial activation and subsequent neuronal damage. *J. Neurochem.* **110**, 1070–1081.

Ghosh S., Dutta K. and Basu A. (2013) Chandipura virus induces neuronal death through Fas-mediated extrinsic apoptotic pathway. *J. Virol.* **87**, 12398–12406.

Gimenez-Barcons M., Clotet B. and Martinez M. A. (2007) Endoribonuclease-prepared short interfering RNAs induce effective and specific inhibition of human immunodeficiency virus type 1 replication. *J. Virol.* **81**, 10680–10686.

Giorgi C., Blumberg B. and Kolakofsky D. (1983) Sequence determination of the (+) leader RNA regions of the vesicular stomatitis virus Chandipura, Cocal, and Piry serotype genomes. *J. Virol.* **46**, 125–130.

Greenspan P., Mayer E. P. and Fowler S. D. (1985) Nile red: a selective fluorescent stain for intracellular lipid droplets. *J. Cell. Biol.* **100**, 965–973.

Grove J. and Marsh M. (2011) The cell biology of receptor-mediated virus entry. *J. Cell. Biol.* **195**, 1071–1082.

Gurav Y. K., Tandale B. V., Jadi R. S., Gunjikar R. S., Tikute S. S., Jamgaonkar A. V., Khadse R. K., Jalgaonkar S. V., Arankalle V. A. and Mishra A. C. (2010) Chandipura virus encephalitis outbreak among children in Nagpur division, Maharashtra, 2007. *Indian J. Med. Res.* **132**, 395–399.

Hirsch-Reinshagen V., Zhou S., Burgess B. L., Bernier L., McIsaac S. A., Chan J. Y., Tansley G. H., Cohn J. S., Hayden M. R. and Wellington C. L. (2004) Deficiency of ABCA1 impairs apolipoprotein E metabolism in brain. *J. Biol. Chem.* **279**, 41197–41207.

Iannacone M., Moseman E. A., Tonti E., Bosurgi L., Junt T., Henrickson S. E., Whelan S. P., Guidotti L. G. and von Andrian U. H. (2010) Subcapsular sinus macrophages prevent CNS invasion on peripheral infection with a neurotropic virus. *Nature* **465**, 1079–1083.

Jadi R. S., Sudeep A. B., Kumar S., Arankalle V. A. and Mishra A. C. (2010) Chandipura virus growth kinetics in vertebrate cell lines, insect cell lines & embryonated eggs. *Indian J. Med. Res.* **132**, 155–159.

Jan J. T., Chatterjee S. and Griffin D. E. (2000) Sindbis virus entry into cells triggers apoptosis by activating sphingomyelinase, leading to the release of ceramide. *J. Virol.* **74**, 6425–6432.

Karasinska J. M. and Hayden M. R. (2011) Cholesterol metabolism in Huntington disease. *Nat. Rev.* **7**, 561–572.

Kendall S. L., Anderson C. F., Nath A., Turchan-Cholewo J., Land C. L., Mactutus C. F. and Booze R. M. (2005) Gonadal steroids differentially modulate neurotoxicity of HIV and cocaine: testosterone and ICI 182,780 sensitive mechanism. *BMC Neurosci.* **6**, 40.

Kilsdonk E. P., Yancey P. G., Stoudt G. W., Bangerter F. W., Johnson W. J., Phillips M. C. and Rothblat G. H. (1995) Cellular cholesterol efflux mediated by cyclodextrins. *J. Biol. Chem.* **270**, 17250–17256.

Kim J., Basak J. M. and Holtzman D. M. (2009) The role of apolipoprotein E in Alzheimer's disease. *Neuron* **63**, 287–303.

Kolsch H., Lutjohann D., Tulke A., Bjorkhem I. and Rao M. L. (1999) The neurotoxic effect of 24-hydroxycholesterol on SH-SY5Y human neuroblastoma cells. *Brain Res.* **818**, 171–175.

Kucherak O. A., Oncul S., Darwich Z., Yushchenko D. A., Arntz Y., Didier P., Mely Y. and Klymchenko A. S. (2010) Switchable nile red-based probe for cholesterol and lipid order at the outer leaflet of biomembranes. *J. Am. Chem. Soc.* **132**, 4907–4916.

Kumar K., Rajasekharan S., Gulati S., Rana J., Gabrani R., Jain C. K., Gupta A., Chaudhary V. K. and Gupta S. (2013) Elucidating the interacting domains of chandipura virus nucleocapsid protein. *Adv. Virol.* **2013**, 594319.

Lahiri D. K. (2004) Apolipoprotein E as a target for developing new therapeutics for Alzheimer's disease based on studies from protein, RNA, and regulatory region of the gene. *J. Mol. Neurosci.* **23**, 225–233.

Mackenzie J. M., Khromykh A. A. and Parton R. G. (2007) Cholesterol manipulation by West Nile virus perturbs the cellular immune response. *Cell Host Microbe* **2**, 229–239.

Matsuda A., Nagao K., Matsuo M., Kioka N. and Ueda K. (2013) 24(S)-hydroxycholesterol is actively eliminated from neuronal cells by ABCA1. *J. Neurochem.* **126**, 93–101.

Mayoral R., Molla B., Flores J. M., Bosca L., Casado M. and Martin-Sanz P. (2008) Constitutive expression of cyclo-oxygenase 2 transgene in hepatocytes protects against liver injury. *Biochem. J.* **416**, 337–346.

Menghani S., Chikhale R., Raval A., Wadibhasme P. and Khedekar P. (2012) Chandipura Virus: an emerging tropical pathogen. *Acta Trop.* **124**, 1–14.

Michikawa M., Fan Q. W., Isobe I. and Yanagisawa K. (2000) Apolipoprotein E exhibits isoform-specific promotion of lipid efflux from astrocytes and neurons in culture. *J. Neurochem.* **74**, 1008–1016.

Mondal A., Roy A., Sarkar S., Mukherjee J., Ganguly T. and Chattopadhyay D. (2012) Interaction of chandipura virus N and P proteins: identification of two mutually exclusive domains of N involved in interaction with P. *PLoS ONE* **7**, e34623.

Movsesyan V. A., Yakovlev A. G., Dabaghyan E. A., Stoica B. A. and Faden A. I. (2002) Ceramide induces neuronal apoptosis through the caspase-9/caspase-3 pathway. *Biochem. Biophys. Res. Commun.* **299**, 201–207.

Mukherjee S., Raghuraman H. and Chattopadhyay A. (2007) Membrane localization and dynamics of Nile Red: effect of cholesterol. *Biochim. Biophys. Acta* **1768**, 59–66.

Nair S., Michaelsen-Preusse K., Finsterbusch K. *et al.* (2014) Interferon regulatory factor-1 protects from fatal neurotropic infection with vesicular stomatitis virus by specific inhibition of viral replication in neurons. *PLoS Pathog.* **10**, e1003999.

Nakai Y. and Kamiguchi H. (2002) Migration of nerve growth cones requires detergent-resistant membranes in a spatially defined and substrate-dependent manner. *J. Cell. Biol.* **159**, 1097–1108.

Ngo M. and Ridgway N. D. (2009) Oxysterol binding protein-related Protein 9 (ORP9) is a cholesterol transfer protein that regulates Golgi structure and function. *Mol. Biol. Cell* **20**, 1388–1399.

Ogawa K., Hishiki T., Shimizu Y., Funami K., Sugiyama K., Miyanari Y. and Shimotohno K. (2009) Hepatitis C virus utilizes lipid droplet for production of infectious virus. *Proc. Jpn. Acad., Ser. B, Phys. Biol. Sci.* **85**, 217–228.

Ohtani Y., Irie T., Uekama K., Fukunaga K. and Pitha J. (1989) Differential effects of alpha-, beta- and gamma-cyclodextrins on human erythrocytes. *Eur. J. Biochem.* **186**, 17–22.

Perera R., Riley C., Isaac G., Hopf-Jannasch A. S., Moore R. J., Weitz K. W., Pasa-Tolic L., Metz T. O., Adamec J. and Kuhn R. J. (2012) Dengue virus infection perturbs lipid homeostasis in infected mosquito cells. *PLoS Pathog.* **8**, e1002584.

Perry R. J. and Ridgway N. D. (2006) Oxysterol-binding protein and vesicle-associated membrane protein-associated protein are required for sterol-dependent activation of the ceramide transport protein. *Mol. Biol. Cell* **17**, 2604–2616.

Pfrieger F. W. (2003) Outsourcing in the brain: do neurons depend on cholesterol delivery by astrocytes? *BioEssays* **25**, 72–78.

Pfrieger F. W. and Ungerer N. (2011) Cholesterol metabolism in neurons and astrocytes. *Prog. Lipid Res.* **50**, 357–371.

Pitha J., Irie T., Sklar P. B. and Nye J. S. (1988) Drug solubilizers to aid pharmacologists: amorphous cyclodextrin derivatives. *Life Sci.* **43**, 493–502.

Poirier J., Baccichet A., Dea D. and Gauthier S. (1993) Cholesterol synthesis and lipoprotein reuptake during synaptic remodelling in hippocampus in adult rats. *Neuroscience* **55**, 81–90.

Prevost M. and Raussens V. (2004) Apolipoprotein E-low density lipoprotein receptor binding: study of protein-protein interaction in rationally selected docked complexes. *Proteins* **55**, 874–884.

Rothwell C., Lebreton A., Young Ng. C., Lim J. Y., Liu W., Vasudevan S., Labow M., Gu F. and Gaither L. A. (2009) Cholesterol biosynthesis modulation regulates dengue viral replication. *Virology* **389**, 8–19.

Stoica B. A., Movsesyan V. A., Lea P. M. 4th and Faden A. I. (2003) Ceramide-induced neuronal apoptosis is associated with dephosphorylation of Akt, BAD, FKHR, GSK-3beta, and induction of the mitochondrial-dependent intrinsic caspase pathway. *Mol. Cell Neurosci.* **22**, 365–382.

Sun X. and Whittaker G. R. (2003) Role for influenza virus envelope cholesterol in virus entry and infection. *J. Virol.* **77**, 12543–12551.

Talekar A., Pessi A. and Porotto M. (2011) Infection of primary neurons mediated by nipah virus envelope proteins: role of host target cells in antiviral action. *J. Virol.* **85**, 8422–8426.

Taniwaki T., Yamada T., Asahara H., Ohyagi Y. and Kira J. (1999) Ceramide induces apoptosis to immature cerebellar granule cells in culture. *Neurochem. Res.* **24**, 685–690.

Vance J. E. and Hayashi H. (2010) Formation and function of apolipoprotein E-containing lipoproteins in the nervous system. *Biochim. Biophys. Acta* **1801**, 806–818.

de Vries H., Schrage C. and Hoekstra D. (1998) An apical-type trafficking pathway is present in cultured oligodendrocytes but the sphingolipid-enriched myelin membrane is the target of a basolateral-type pathway. *Mol. Biol. Cell* **9**, 599–609.

Yamanaka K., Saito Y., Yamamori T., Urano Y. and Noguchi N. (2011) 24(S)-hydroxycholesterol induces neuronal cell death through necroptosis, a form of programmed necrosis. *J. Biol. Chem.* **286**, 24666–24673.

Yamanaka K., Urano Y., Takabe W., Saito Y. and Noguchi N. (2014) Induction of apoptosis and necroptosis by 24(S)-hydroxycholesterol is dependent on activity of acyl-CoA:cholesterol acyltransferase 1. *Cell Death Dis.* **5**, e990.